Preferential Occupation of Xenon in Zeolite MCM-22 As Revealed by 129Xe NMR Spectroscopy

ARTICLE *in* THE JOURNAL OF PHYSICAL CHEMISTRY B · OCTOBER 2001

Impact Factor: 3.3 · DOI: 10.1021/jp011710+

6 AUTHORS, INCLUDING:

Feng Deng
Xi'an Jiaotong University
297 PUBLICATIONS **4,764** CITATIONS
SEE PROFILE

Mojie Cheng
Dalian Institute of Chemical Physics
86 PUBLICATIONS **1,760** CITATIONS
SEE PROFILE

Ye Chaohui
Chinese Academy of Sciences
144 PUBLICATIONS **1,846** CITATIONS
SEE PROFILE

Preferential Occupation of Xenon in Zeolite MCM-22 As Revealed by ^{129}Xe NMR Spectroscopy

Fang Chen,[†] Feng Deng,*[,†] Mojie Cheng,[‡] Yong Yue,*[,†] Chaohui Ye,[†] and Xinhe Bao[‡]

State Key Laboratory of Nuclear Magnetic Resonance and Atomic and Molecular Physics, Wuhan Institute of Physics and Mathematics, The Chinese Academy of Sciences, Wuhan 430071, P. R. China, and State Key Laboratory of Catalysis, Dalian Institute of Chemical Physics, The Chinese Academy of Sciences, Dalian 116023, P. R. China

Received: May 4, 2001; In Final Form: July 16, 2001

Adsorption of xenon in zeolite MCM-22, a zeolite containing two separate pore systems (the 10-membered ring (MR) sinusoidal channels and 12-MR supercages interconnected by 10-MR window system), has been investigated in detail with ^{129}Xe NMR spectroscopy as a function of Xe loadings over a wide range of temperatures (120−350 K). NMR results suggest that Xe atoms are preferentially adsorbed in the supercages of the zeolite at low Xe pressure (less than a few atmospheres), while Xe atoms can penetrate into the two-dimensional sinusoidal channels at high Xe pressure. No direct exchange between the Xe in the supercages and the sinusoidal channels was observed in variable-temperature (VT) ^{129}Xe NMR experiments for all of the samples, which is in line with the crystal structure of the zeolite. However, when the Xe adsorption pressure is greater than 6 atm, two different kinds of Xe exchange were observed in VT experiments over the temperature range. The exchange of Xe at the different adsorption sites in the same supercage (i.e., Xe atoms in the two pockets and those in the central part of the supercage) occurs at lower temperatures (170−122 K), which is demonstrated by two-dimensional ^{129}Xe NMR exchange spectroscopy. The exchange between Xe in the supercage and the sinusoidal channel takes place through gaseous Xe in the interparticle space at higher temperatures (280−350 K).

Introduction

Zeolites are crystalline microporous materials consisting of SiO_4 and AlO_4 tetrahedra that are linked together in three-dimensional networks of pores and cages of varying sizes. They contain exchangeable cations that balance the framework negative charges arising from Al in the structure. Zeolites are now largely used as adsorbents and as catalysts in the chemical and the petrochemical industries. After the big catalytic success of 10-membered ring (MR) zeolites with intersecting pores, such as ZSM-5 that can selectively transform molecules with a diameter less than 0.7 nm, there has been a tendency to synthesize zeolite catalysts that contain intersecting channels with pores that are both large (12-MR) and medium (10-MR) in size.[1,2] Such a combination in one zeolite structure could enable the large pores to convert large molecules and the medium pores to gain shape selectivity. Synthetic materials such as NU-87 and SSZ-26 have 10- and 12-MR pore systems.[3,4] However, in the former, the access to the inside is somewhat restricted, while in the latter, it is likely to offer a particular combination of activity and selectivity as an acid catalyst. A new zeolite, MCM-22, may be another choice for this purpose. It is of great interest to study the adsorption and the catalytic properties of these zeolites.

MCM-22, invented by Mobil in 1990, is a novel zeolite molecular sieve that has a unique and unusual crystal structure.[5−7]

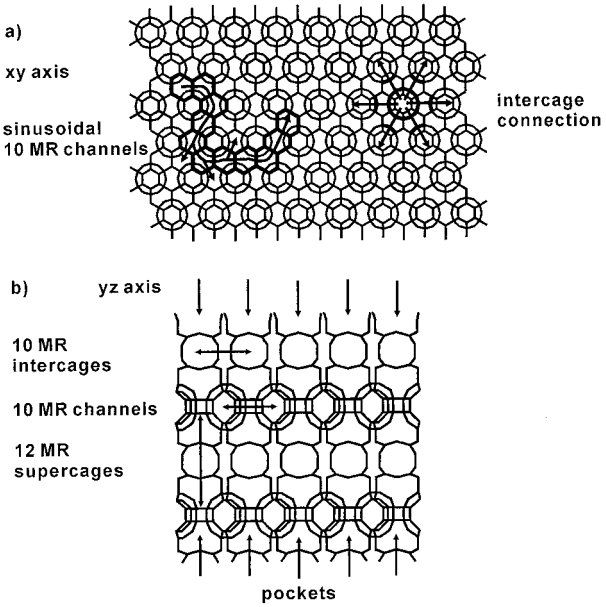

Figure 1. Schematic view of the independent pore systems in MCM-22: (a) The sinusoidal 10-MR channels are all interconnected to each other. (b) The large cavities are the 12-MR supercage, which are interconnected through short 10-MR conduits.

Its internal structure is composed of two different independent pore systems (see Figure 1): the 10-MR two-dimensional (2D) sinusoidal channels and the 12-MR large supercages (0.71 × 0.71 × 1.82 nm) interconnected by the 10-MR window systems. The free diameters of these apertures are 0.4 × 0.59 nm for the sinusoidal channel and 0.4 × 0.54 nm for the entrance to the

* Corresponding authors. E-mail: dengf@wipm.whcnc.ac.cn and yueyong@wipm.whcnc.ac.cn. Fax: 86-27-87885291.

[†] Wuhan Institute of Physics and Mathematics, The Chinese Academy of Sciences.

[‡] Dalian Institute of Chemical Physics, The Chinese Academy of Sciences.

10.1021/jp011710+ CCC: $20.00
Published on Web 09/11/2001

supercage. There is no communication between the two pore systems and, consequently, no access to the internal pore along the *c* direction through the top or bottom surface of the crystal plates. As revealed by Lawton et al.,[8] a certain number of external zeolitic pockets (with 12-MR openings and having a depth of ca. 0.7 nm) cover the hexagonal faces of the crystals, which may play an important role in certain catalytic processes. However, it can be seen from Figure 1 that the concentration of the surface pockets is strongly dependent on the thickness of the crystal in the *c* direction.

MCM-22 has a high thermal stability (up to 1198 K), a high BET surface area (>400 m^2/g), and a very large sorption capacity for water and small organic molecules.[2,9] It has shown an interesting potential to act as a catalyst in chemical and petrochemical processes,[10−13] such as cracking, alkylation, isomerization, and conversion of paraffin to olefin. Although MCM-22 contains both 10- and 12-MR, many studies have shown that, for certain catalytic processes, it behaves more like a 12-MR zeolite than a 10-MR zeolite.[13−15] While it is recognized that the large 12-MR supercages may accommodate larger intermediates and thus explain some of these behaviors, the 10-MR openings associated with the cage will restrict the diffusion of reactants or products. Lawton et al.[8] studied an MCM-22 zeolite of very small crystallites (having 5−10 nm thickness, ca. 2−3 layers of supercages, and two layers of surface pockets in the *c* direction) and they considered the surface 12-MR pockets to be a viable alternative for a reaction site. It is still unclear which pore system, the 12-MR supercage or the 10-MR sinusoidal channel inside the MCM-22 crystals, is the preferred adsorption site and if the latter is easily accessible by adsorbed molecules.

NMR is a powerful tool for the identification of the short-range order and the local structure of zeolites. Solid-state NMR has been employed to study the Si and Al distribution and the dealumination as well as the acidity of MCM-22.[7,16−19] It is reported that seven Si sites and three Al sites were observed in the corresponding ^{29}Si and ^{27}Al magic-angle spinning (MAS) NMR spectra and were assigned to different crystallographically inequivalent framework atoms. ^{129}Xe is an ideal NMR probe atom for investigating the microstructure of porous materials, having favorable properties (with spin $I = {}^1/_2$ and a relatively high NMR sensitivity) as well as being inert and small enough (with a diameter of 0.44 nm) to fit into the zeolite pores. The chemical shifts of ^{129}Xe are very sensitive to the pore geometry and the chemical surroundings. Since the discoveries of Ito and Fraissard,[20] ^{129}Xe NMR spectroscopy has been widely used to study zeolites and related molecular sieves, mineral clays, and so forth.[21−26] However, to the best of our knowledge, few studies of zeolite MCM-22 have been carried out by ^{129}Xe NMR spectroscopy.

In the present work, we attempted to examine the unique and unusual pore structure of MCM-22 zeolite by ^{129}Xe NMR spectroscopy. Consequently, we measured the ^{129}Xe chemical shifts with different Xe loadings and investigated the exchange of Xe adsorbed in the zeolite over a wide temperature range (120−350 K).

Experimental Section

Sample Preparation. MCM-22 zeolite was synthesized according to the procedures described in the literature,[5,27] using hexamethyleneimine (HMI) as a structure-directing agent. The synthesis mixtures were prepared using silica sol (26.5 wt % SiO_2), sodium aluminate, HMI, sodium hydroxide, and deionized water. Sodium hydroxide (0.8 g) and sodium aluminate (1.7 g) were dissolved in 135 g of deionized water, and then 10.3 g of HMI and 46.8 g of silica sol were added with stirring. The molar compositions of the resulting mixtures were 13.5 Na_2O, 5 Al_2O_3, 100 SiO_2, 4500 H_2O, and 50 HMI. After aging and stirring for 60 min at room temperature (RT), the mixture was transferred into a Teflon-lined autoclave and heated to 423 K for 96 h. The crystalline product was filtered, washed with deionized water until it reached a pH < 9, and then dried at 353 K overnight. The sample was calcined at 810 K for 24 h to remove the template. After a 3-fold successive exchange of the sample with 1 M NH_4NO_3, it was calcined at 773 K for 4 h and the H form of MCM-22 was obtained. The crystal size of the sample obtained under these conditions was about 5−10 μm in diameter and about 1 μm in thickness. A sample of HMCM-22 with Si/Al = 20 was synthesized according to the above procedure. The MCM-22 zeolite exhibits a typical MCM-22 crystalline structure (MWW, IZA code), as suggested by X-ray diffraction (XRD), and no intensities of other crystallites have been observed. N_2 adsorption isotherm measurement indicates that no secondary pores are present in the sample.

Samples for ^{129}Xe NMR measurements were prepared as follows. A known amount of HMCM-22 was placed in a glass tube with an 8 mm outside diameter and packed closely to a bed length of about 20 mm. The tube was connected to a vacuum line. The temperature was gradually increased at a rate of 1 °C/min, and the sample was kept at the final temperature of 400 °C at a pressure below 10^{-3} Pa over a period of 12 h and then cooled. After the sample cooled to ambient temperature, a measured volume of Xe gas (^{129}Xe 26.24%) with a known pressure was condensed and frozen inside the sample by cooling the sample region of the NMR tube with liquid nitrogen. Finally, the NMR tube was flame sealed. The amount of adsorbed Xe can be easily calculated as the number of Xe atoms per gram of the sample. Because there are 72 T atoms per supercage, the amount of adsorbed Xe can also be expressed as the number of Xe atoms/supercage for samples with lower Xe pressure, in which Xe atoms are preferentially adsorbed in the supercage (see the following).

NMR Spectroscopy. RT ^{129}Xe NMR spectra were acquired using a Varian 200 spectrometer modified with a Tecmag system at a frequency of 55.34 MHz. A 13 μs ($\pi/2$) excitation pulse and a 0.5 s recycle delay were employed to record ^{129}Xe NMR spectra. Spin−lattice relaxation time (T_1) was measured using an inversion−recovery pulse sequence. The T_1 of the adsorbed Xe is usually less than 50 ms. Variable-temperature (VT) experiments were carried out on a Bruker WP-80 spectrometer at a frequency of 22.17 MHz. The samples were cooled in steps from RT to 120 K or warmed in steps from RT to 350 K at a rate of approximately 1−2 K/min, being allowed to equilibrate at a desired temperature for 10−20 min before data acquisition.

Two-dimensional ^{129}Xe NMR exchange experiments were performed at 145 K using a $90°-t_1-90°-t_m-90°-t_2$ pulse sequence.[28,29] The 2D NMR data were acquired with 32 and 512 points in the t_1 and t_2 dimensions, respectively. Before Fourier transform, the t_1 dimension was zero-filled to 256 points. The mixing time (t_m) was varied from 0.1 to 4 ms. The spectra were displayed in the absolute value mode.

We measured the ^{129}Xe chemical shift, at RT, of an external-standard sample of Xe gas at 6.3 atm with a small amount of oxygen prior to each set of measurements. The shift was then corrected to zero pressure with the equations given by Jameson et al.[30,31]

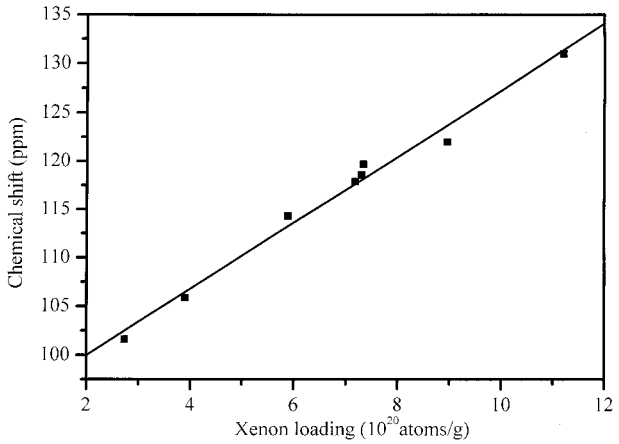

Figure 2. Variation of the ^{129}Xe NMR chemical shift at room temperature versus the Xe concentration for the HMCM-22 zeolite with a Si/Al of 20.

Results and Discussion

^{129}Xe NMR Chemical Shifts at RT. Only a single symmetrical resonance is observed in the ^{129}Xe NMR spectra acquired at RT when the adsorption pressure of Xe is varied below 2 atm, indicating that the Xe atoms may be adsorbed only in one set of pores. However, at present, we are unable to determine if the resonance is the result of a rapid exchange of Xe between different sorption sites. As will be seen in the following, this possibility can be ruled out by VT ^{129}Xe NMR experiments. Figure 2 shows the ^{129}Xe chemical shift variation as a function of the Xe loadings at RT. A linear increase of the chemical shifts is evident when the Xe loading is varied from 2.8 to 11 $\times$ 10^{20} atoms/g or the Xe pressure from 30 to 506 Torr, which is in line with the characteristics of univalent ionic-type zeolites (such as H^+, Li^+, and Na^+).[22,23]

For H-form zeolites at RT, the chemical shifts of adsorbed Xe is the sum of three terms at low xenon pressure:[23]

$$\delta = \delta_0 + \delta_s + \delta_{Xe-Xe}\rho_{Xe} \quad (1)$$

where δ_0 is the reference (gaseous Xe at zero pressure); δ_s arises from collisions between Xe and the surface of the zeolitic pores (it depends on the free path of the Xe atoms in the pores and reflects the information on zeolite structure); and $\delta_{Xe-Xe}\rho_{Xe}$ is due to Xe$-$Xe collisions (it is expected to vary linearly with the local Xe concentrations and becomes predominant at high Xe pressure).

By fitting the data in Figure 2 with eq 1, we can obtain that the Xe chemical shift (δ_s), extrapolated to zero Xe loading, is 93 ppm. δ_s has been related to the size and shape of the internal cavity by means of the mean free path ($\bar{l}$) of adsorbed Xe imposed by the zeolite structure. Generally, the larger the dimensions of the cavity containing Xe, the smaller the value of δ_s. The final correlation suggested by Demarquay and Fraissard[32] is as follows:

$$\delta_s = 243\frac{2.054}{2.054 + \bar{l}} \quad (2)$$

We can obtain that the mean free path of Xe adsorbed in HMCM-22 is $\bar{l} = 0.33$ nm by eq 2. As is well-known, it is easy to calculate the exact value of $\bar{l}$ for Xe in a sphere or an infinite cylinder. In other cases, no analytical solution for $\bar{l}$ is available. For a sphere of diameter (D_s), the mean free path is $\bar{l} = (D_s - 0.44)/2$, while for an infinite cylinder (D_c), we have $\bar{l} = D_c - 0.44$ (taking the diameter of Xe to be 0.44 nm). As stated earlier, the free diameters of the sinusoidal channel and the supercage are 0.4 $\times$ 0.59 and 0.71 $\times$ 0.71 nm, respectively, and the inner height of the supercage is 1.8 nm. If the sinusoidal channels are approximated to infinite cylinders, the corresponding maximum mean free path would be $\bar{l} = 0.15$ nm (0.59 $-$ 0.44 nm), much smaller than that determined from ^{129}Xe NMR. Indeed, $\bar{l}$ of Xe in the sinusoidal channel is expected to be smaller than 0.15 nm because of the high degree of tortuosity in the circular channel that will affect the mobility of Xe. If the supercages are approximated to spheres with a diameter ranging from 0.71 to 1.82 nm, then the corresponding $\bar{l}$ would be in the range of 0.135$-$0.68 nm, much closer to the experimental value. The previous experimental and theoretical works have already demonstrated that the diffusion of hydrocarbons, such as benzene or propylene, is much more effective in the supercage than in the sinusoidal channel, which was attributed to the high degree of tortuosity of the latter.[1,33$-$35] Thus, we conclude that Xe atoms are preferentially adsorbed in the supercages of zeolite MCM-22 at low pressures. The amount of Xe adsorbed in the supercage changes from 2.1 to 8.0 atoms/cage when the Xe pressure varies from 30 to 506 Torr.

As mentioned above, the external surface of the MCM-22 crystals is covered with 12-MR pockets (each of which is half of a supercage), having a depth of approximately 0.7 nm and a diameter of around 0.7 nm. It is difficult to estimate the mean free path of Xe in the pockets of the zeolite. However, preferential occupation of Xe in the surface pockets can be excluded at low Xe pressure. Because the size of our MCM-22 zeolite crystallite is very large (having a thickness of about 1 μm in the *c* direction), it can be estimated that about 400 layers of the supercages are present in the *c* direction, while there are only two layers of the pockets on the external surface. Thus, the concentration of the surface pockets is very low and can be neglected with respect to those of the supercages and the sinusoidal channels in our MCM-22 sample. Of course, a small number of Xe atoms may be trapped in the surface pockets or the sinusoidal channels at low Xe pressure. However, their concentrations should be too low to be detected by ^{129}Xe NMR.

VT ^{129}Xe NMR. *At Low Xe Pressure.* Temperature-dependent ^{129}Xe NMR spectra of samples with low Xe pressures (<1 atm) are similar. Figure 3 shows a typical result for a sample with a Xe pressure of 506 Torr (or 8.0 Xe atoms/supercage). Only one symmetrical resonance is observed, and the line width decreases first and then increases when the temperature varies from 350 to 120 K. This indicates again that only one set of the pores is accommodated by Xe, and no exchange of Xe between different cavities occurs over the temperature range. The chemical shifts increase from 115 to 197 ppm when the temperature decreases from 350 to 120 K. This is a general trend in VT ^{129}Xe NMR experiments because of the increase in both the Xe concentration (ρ_{Xe}) and δ_s at low temperatures. Even when the adsorption pressure increases to 2 atm, only a symmetrical resonance (not shown) is observed over the temperature range, though its chemical shift varies with the temperature.

The VT ^{129}Xe NMR experiments over a temperature range of 120$-$350 K suggest that Xe atoms are preferentially trapped inside the supercages when the adsorption pressure of Xe is varied below 2 atm. While under these conditions, the sinusoidal channel system apparently does not allow access to the small spheric Xe atoms (0.44 nm) because of its high degree of tortuosity. Many studies have shown that the MCM-22 behaves more like a 12-MR zeolite than a 10-MR zeolite for certain catalytic processes,[13$-$15] probably implying that the 12-MR supercage is the reaction site and that the 10-MR channel is

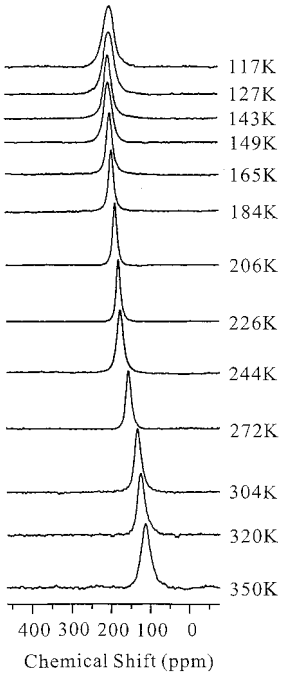

Figure 3. Temperature-dependent ^{129}Xe NMR spectra of Xe adsorbed in the HMCM-22 zeolite with a Xe pressure of 506 Torr (a Xe loading of 1.1×10^{21} atoms/g or 8.0 atoms/supercage). The temperature is varied from 117 to 350 K. Only one symmetrical resonance was observed over the temperature range.

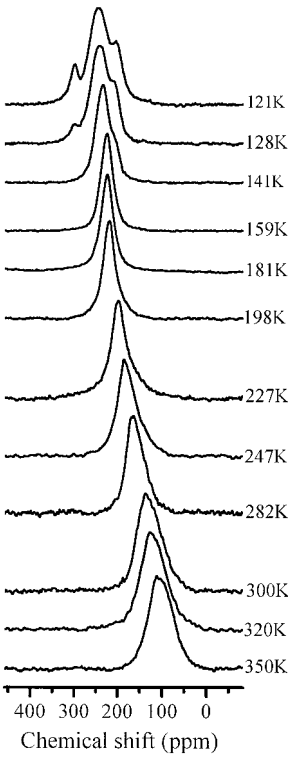

Figure 4. Temperature-dependent ^{129}Xe NMR spectra of Xe adsorbed in the HMCM-22 zeolite with a Xe pressure of 6.0 atm (or a Xe loading of 1.8×10^{21} atoms/g). The temperature is varied from 121 to 350 K.

difficult for the reactants to access. The present VT ^{129}Xe NMR results provide direct evidence that the supercage may be a preferred adsorption (or reaction) site in MCM-22 zeolite. One could speculate that it is difficult for hydrocarbon molecules with a diameter larger than 0.44 nm, such as benzene (0.58 nm), to penetrate into the 10-MR channels under the same conditions. Indeed, we also measured the ^{129}Xe NMR spectrum of a MCM-22 sample with coadsorption of benzene and Xe and observed only one resonance, probably resulting from the Xe atoms that are associated with benzene trapped in the supercages. The adsorption and diffusion of benzene in MCM-22 at 650 K were studied recently by Hou et al.[35] using molecular dynamics and Monte Carlo methods, and they revealed that the diffusion and mobility of benzene mainly happened in the 12-MR supercages, where there were three preferred adsorption sites of benzene. A detailed study of the adsorption of various hydrocarbon molecules in MCM-22 zeolite by ^{129}Xe NMR is still in progress.

At High Xe Pressure. Figure 4 shows the VT ^{129}Xe NMR spectra of HMCM-22 at a Xe pressure of 6.0 atm. A symmetrical resonance is observed when the temperature is changed from 159 to 350 K. However, the line width of the signal is largely broadened when the temperature increases above 300 K, which is not observed in the samples with lower Xe pressures. This may result from an exchange of Xe in the supercage with the gaseous Xe in the interparticle space, which is likely to cause a fluctuation in the number of Xe in the supercage.[36] This number fluctuates as Xe atoms move in and out of each cage. Because the chemical shift of the Xe atoms in a given cage depends on the number of Xe atoms in that cage, one would observe a large inhomogeneous broadening (or a chemical shift distribution) resulting from the fluctuation. The amount of adsorbed Xe can be estimated to be 11.7 atoms/cage, assuming that all of the Xe atoms are trapped in the supercages.

It is surprising that a new signal at 205 ppm appears as a shoulder on the high-field region of the main peak (235 ppm) at 141 K. A further decrease in temperature to 128 K causes the appearance of a small signal at 304 ppm, which can be tentatively assigned to excess Xe frozen on the exterior surface of the zeolite microcrystallites.[36]

Cheung et al.[36] found that the line shape of the ^{129}Xe resonance of the NaY zeolite at 144 K depended on the rate at which the sample was cooled to that temperature. In the case of rapid cooling (samples were cooled from 164 to 144 K as quickly as possible), they observed complicated ^{129}Xe NMR spectra, having different peaks with different chemical shifts. It took about 10^3 s for all of the spectral components to converge to a single, sharp line at 144 K. The authors concluded that the various resonances were associated with different Xe densities across the samples, giving rise to a distribution of chemical shifts. Equilibrium was eventually established when all of the particles had the same Xe density. Such a distribution was also observed by Ratcliffe and Ripmeester[37] for a number of Xe/NaY samples after they were quenched to 77 K from 295 K. These samples took many months to reach equilibrium.

In our VT experiments, we decreased the temperature very slowly (1 K/min) and waited for 10−20 min for the sample to reach equilibrium at a desired temperature prior to data acquisition. Furthermore, for some VT experiments performed at a temperature below 141 K, we repeated the same experiment 2 h later. No obvious change was observed in the two corresponding ^{129}Xe NMR spectra. Thus, the distribution of the chemical shifts caused by a temperature (or a Xe densities) gradient across the samples can be neglected in the case of our samples. The various ^{129}Xe spectral components observed at lower temperatures are associated with different Xe sites. The appearance of the new signal at 205 ppm suggests that a certain kind of fast exchange of Xe is slowed when the temperature is reduced to 141 K.

VT ^{129}Xe NMR spectra of a sample with a high adsorption pressure (8.2 atm) are shown in Figure 5. At least two unresolved signals, a narrow one at 168 ppm resulting from Xe

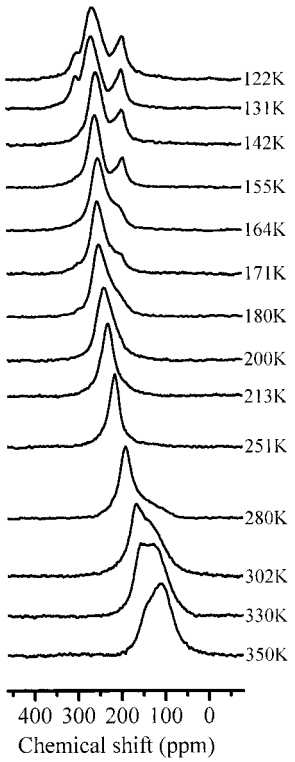

Figure 5. Temperature-dependent ^{129}Xe NMR spectra of Xe adsorbed in the HMCM-22 zeolite with a Xe pressure of 8.2 atm (or a Xe loading of 1.9×10^{21} atoms/g). The temperature is varied from 122 to 350 K.

in the supercages and a broad shoulder in the high-field region, are present in the ^{129}Xe NMR spectrum acquired at 280 K. The line shape looks like a chemical-shift tensor pattern. However, with an increase in the temperature, the intensity of the high-field signal increases at the expense of the low-field signal, indicating that a certain kind of exchange occurs. Rapid exchange for intra- and interparticle Xe predicts the observation of a single line, though its line width will become broadened and its exact chemical shift will depend on the relative amounts of Xe inside and outside of the particles[38] (which has been observed in the VT ^{129}Xe NMR spectra of the sample with a Xe pressure of 6.0 atm; Figure 4). Therefore, the high-field signal should be an independent resonance and may arise from Xe adsorbed in the sinusoidal channels or in the external surface pockets. As mentioned above, the concentration of the surface pockets is very low with respect to that of the sinusoidal channels. The high-field signal should mainly result from the Xe adsorbed in the sinusoidal channels. Its smaller chemical shift can be attributed, at least in part, to the fast exchange between the Xe in the sinusoidal channels and that in the interparticle space. Most likely, more and more Xe atoms diffuse out of the supercages and are trapped in the sinusoidal channels of the MCM-22 zeolite when the temperature increases above 280 K, which can be referred to as a kind of indirect exchange of Xe between the two different pores through the gaseous Xe in the interparticle space.

It is interesting that only a narrow resonance at 215 ppm is present when the sample is cooled to 251 K, implying that the supercages preferentially accommodate Xe at the low temperature. A further decrease in the temperature causes a downfield shift of the narrow resonance and a shoulder at ca. 200 ppm that begins to appear when the sample is cooled to 180 K. Two well-resolved resonances are observed when the temperature is reduced below 155 K. It is evident that a fast exchange of Xe in different adsorption sites is likely to occur over the temperature range of 251−200 K. When the temperature is lower than 155 K, the exchange is slowed, and two resonances of Xe from different sites are well resolved. In principle, the exchange of Xe in different adsorption zones can be studied by 2D ^{129}Xe exchange NMR spectroscopy in the slow-exchange limit.

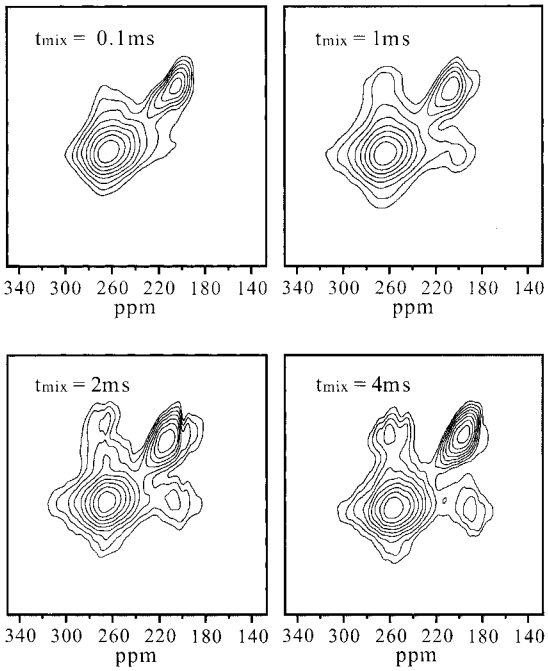

Figure 6. Two-dimensional ^{129}Xe exchange NMR spectra of Xe adsorbed in the HMCM-22 zeolite (with a Xe pressure of 8.2 atm) at different mixing times, which were recorded at 145 K. Cross-peaks become visible and intense at a mixing time of 1 ms, indicating that a certain kind of Xe exchange occurs on the time scale.

2D ^{129}Xe exchange NMR. Two-dimensional NMR exchange spectroscopy, originally introduced by Jeener,[28] has found wide applications in the study of the chemical exchange in the liquid phase, and more recently, some applications to surface and zeolite chemistry have been reported.[24,39−42] The presence of chemical exchange within a time scale of the order of the mixing time (t_m in the pulse sequence) gives rise to cross-peaks in the 2D spectrum between the resonances of the sites in the exchange. Here, we employed 2D NMR exchange spectroscopy to clarify the exchange process of Xe in zeolite HMCM-22. These experiments were carried out at 145 K, giving rise to a strong signal and good resolution. At high temperatures (i.e., 300 K), the two resonances are poorly resolved, and the application of 2D NMR exchange spectroscopy is not feasible.

Figure 6 shows the 2D ^{129}Xe NMR exchange spectra of the sample with a Xe pressure of 8.2 atm as a function of t_m. At short mixing times on the order of 0.1 ms, primarily diagonal peaks corresponding to two distinct adsorption sites are observed. Cross-peaks become visible at $t_m = 1$ ms and intense at $t_m = 2$ or 4 ms. Although the 2D exchange method can provide quantitative information about the exchange rate between different adsorption sites, we are unable to obtain an accurate exchange rate in the present case because of the low resolution achieved. Nevertheless, we can deduce that the exchange of Xe occurs on a time scale of around several milliseconds.

Ripmeester et al.[41] have used ^{129}Xe 2D exchange NMR to study both intra- and interparticle exchange in zeolites and revealed that the Xe exchange between the particles of NaX and NaY zeolites occurs at RT when $t_{mix} \geq 10$ ms, while that between the different adsorption zones of mordenite (i.e., Xe

in the main channels and the side pockets) takes place when $t_{mix} \geq 2$ ms. Obviously, an intraparticle exchange is more efficient than an interparticle one. According to the topological structure of MCM-22, there is no communication between the supercages and sinusoidal channels; thus, Xe atoms cannot exchange directly between the two cavities but can exchange through gaseous Xe in the interparticle space of the zeolite. The exchange rate of Xe in MCM-22 at 145 K is close to the intraparticle exchange rate of Xe in mordenite at ambient temperature. Thus, the exchange of Xe in MCM-22 is expected to be very fast and can be attributed to an intraparticle exchange (direct exchange).

At high Xe pressure and low temperature, Xe atoms are preferentially adsorbed in the supercages. According to the crystal structure of MCM-22, each supercage is connected to another six supercages through 10-MR windows (Figure 1); therefore, the intercage exchange of Xe is, in principle, possible. If the Xe exchange observed at 145 K resulted from the intercage exchange, it is difficult to understand that the Xe atoms, adsorbed in different supercages, would have two different chemical surroundings (or chemical shifts) because each supercage should be completely equivalent. Thus, we tentatively ascribe the Xe exchange observed at 145 K to an intraparticle exchange between the Xe adsorbed in the different zones of the same supercage (i.e., the Xe atoms in the two pockets and those in the central part of the supercage). This kind of exchange is very effective, even at a temperature as low as 122 K. Therefore, two kinds of Xe exchange are observed in the HMCM-22 zeolite: an indirect exchange of Xe at higher temperatures (280−350 K) and a direct exchange at lower temperatures (170−122 K).

It is interesting that decreasing the temperature (170−122 K) causes a redistribution of the Xe atoms in the supercage, which is evidenced by the fact that the high-field signal (at ca. 200 ppm) increases at the expense of the main peak (at 255 ppm; Figure 5) when the temperature is reduced from 180 to 122 K. Generally, the larger the space containing Xe, the smaller the corresponding chemical shift. We tentatively ascribe the high-field signal at ca. 200 ppm to Xe in the central part and the main peak at 255 ppm to Xe in the two pockets of the supercage. The VT experimental result suggests that, at lower temperatures, Xe atoms are more preferentially trapped in the two pockets of the supercage. This phenomenon has not been observed for the samples with low Xe pressures, where only a symmetrical resonance is observed even at a temperature as low as 120 K, indicating that Xe atoms in the supercages still undergo a fast exchange.

Three preferred adsorption sites of benzene in the supercage of the MCM-22 zeolite were found by theoretical simulation:[35] one (site S4) was near the center of the supercage, and the others (S2 and S3) were in the two pockets of the supercage. The benzene molecules located near the S4 site were more energetically unfavorable than those near the S2 and S3 sites. Although we could not find any theoretical studies on the adsorption of Xe in MCM-22, this result may suggest that it is likely to have some preferred adsorption sites in the supercages for certain adsorbed molecules.

Obviously, the lower temperature ^{129}Xe NMR data provide a more detailed description for the Xe adsorption in the MCM-22 zeolite. Our next work is to perform ^{129}Xe NMR experiments at temperatures lower than 120 K.

Conclusions

Our ^{129}Xe NMR data show that Xe atoms are preferentially adsorbed in the supercage of the MCM-22 zeolite when the Xe pressure is below a few atmospheres, while Xe can penetrate into the 2D sinusoidal when the pressure increases to greater than 6 atm because of the high degree of tortuosity (which may partially explain why the MCM-22 behaves more like a 12-MR zeolite than a 10-MR zeolite for certain catalytic processes). No bulk-liquid Xe was found inside the supercage, while bulk-solid Xe presumably formed on the exterior surface of the zeolite particles. We found that two different kinds of Xe exchange are present at high Xe pressure over the temperature range of 122−350 K. The exchange of Xe in the different adsorption sites of the same supercage occurs at lower temperatures (122−170 K). The time scale for the intraparticle exchange is very fast. As revealed by 2D ^{129}Xe exchange spectroscopy, the exchange occurs in less than 1 ms. On the other hand, the exchange of Xe in the supercage with Xe in the interparticle space takes place at higher temperatures (280−350 K). Apparently, the ^{129}Xe NMR results provide some new insights into the adsorption properties of the MCM-22 zeolite.

Acknowledgment. The authors are grateful to the National Science Foundation of China (Grant 29873065) for financial support.

References and Notes

(1) Corma, A.; Corell, C.; Llopis, F.; Martinez, A.; Perez-Pariente, J. *Appl. Catal., A* **1994**, *115*, 121.
(2) Corma, A.; Corell, C.; Fornes, V.; Kolodziejski, W.; Perez-Pariente, J. *Zeolites* **1995**, *15*, 576.
(3) Shanon, M. D. *Nature* **1991**, *353*, 417.
(4) Zones, S. I.; Santilli, D. S.; Ziemer, J. N.; Holtermann, D. L.; Pecoraro, T. A.; Innes, R. A. U.S. Patent 4,910,006, 1990.
(5) Rubin, M. K.; Chu, P. U.S. Patent 4,954,325, 1990.
(6) Leonowicz, M. E.; Lawton, J. A.; Lawton, S. L.; Rubin, M. K. *Science* **1994**, *264*, 1910.
(7) Kennedy, G. J.; Lawton, S. L.; Rubin, M. K. *J. Am. Chem. Soc.* **1994**, *116*, 11000.
(8) Lawton, S. L.; Leonowicz, M. E.; Partridge, R. D.; Chu, P.; Rubin, M. K. *Microporous Mesoporous Mater.* **1998**, *23*, 109.
(9) Kolodziejski, W.; Zicovich-Wilson, C.; Corell, C.; Perez-Pariente, J.; Corma, A. *J. Phys. Chem.* **1995**, *99*, 7002.
(10) Verhoef, M. J.; Creyghton, E. J.; Peters, J. A.; van Bekkum, H. *Chem. Commun.* **1997**, 1989.
(11) Wu, P.; Komastsu, T.; Yashima, T. *Microporous Mesoporous Mater.* **1998**, *22*, 343.
(12) Corma, A.; Martinez-Triguero, J. *J. Catal.* **1997**, *165*, 102.
(13) Souverijns, W.; Verrelst, W.; Vanbutsele, G.; Martens, J. A.; Jacobs, P. A. *J. Chem. Soc., Chem. Commun.* **1994**, 1671.
(14) Ravishankar, R.; Bhattacharya, D.; Jacob, N. E.; Sivasanker, S. *Microporous Mater.* **1995**, *4*, 83.
(15) Perego, C.; Amarilli, S.; Millini, R.; Bellussi, G.; Girotti, G.; Terzoni, G. *Microporous Mater.* **1996**, *6*, 395.
(16) Lawton, S. L.; Fung, A. S.; Kennedy, G. L.; Alemany, L. B.; Chang, C. D.; Hatzikos, G. H.; Lissy, D. N.; Rubin, M. K.; Tinken, H. C.; Steuernagel, S.; Woessner, D. E. *J. Phys. Chem.* **1996**, *100*, 3788.
(17) Hunger, M.; Ernst, S.; Weitjamp, J. *Zeolites* **1995**, *15*, 188.
(18) Kennedy, G. L.; Lawton, S. L.; Fung, A. S.; Rubin, M. K.; Steuernagel, S. *Catal. Today* **1999**, *49*, 385.
(19) Ma, D.; Deng, F.; Fu, R. Q.; Han, X. W.; Bao, X. H. *J. Phys. Chem. B* **2001**, *105*, 1770.
(20) Ito, T.; Fraissard, J. In *Proceedings of the 5th International Conference on Zeolites*, Naples, Italy, 1980; Rees, L. V., Ed.; Heyden: London, 1980; p 510.
(21) Ryoo, R.; Cho, S. J.; Pak, C.; Kim, J. G.; Ihm, S. K.; Lee, J. Y. *J. Am. Chem. Soc.* **1992**, *114*, 76.
(22) Barrie, P. J.; Klinowski, J. *Prog. Nucl. Magn. Reson. Spectrosc.* **1992**, *24*, 91.
(23) Bonardet, J. L.; Fraissard, J.; Dedeon, A.; Springuel-Huet, M. A. *Catal. Rev.—Sci. Eng.* **1999**, *41*, 115.
(24) Grosse, Rs.; Burmeister, R.; Boddenberg, B. *J. Phys. Chem.* **1991**, *95*, 2443.
(25) Labouriau, A.; Pietrass, T.; Weber, W. A.; Gates, B. C.; Earl, W. L. *J. Phys. Chem. B* **1999**, *103*, 4323.
(26) Labouriau, A.; Panjabi, G.; Enderle, B.; Pietrass, T.; Gattes, B. C.; Earl, W. L.; Ott, K. C. *J. Am. Chem. Soc.* **1999**, *121*, 7674.
(27) Corma, A.; Corell, C.; Perez-Pariente, J. *Zeolites* **1995**, *15*, 2.

(28) Jeener, J.; Meier, B. H.; Bachmann, P.; Ernst, R. R. *J. Chem. Phys.* **1979**, *71*, 4546.
(29) Bax, A. *Two-Dimensional Nuclear Magnetic Resonance in Liquids*; Delft University Press: Delft, The Netherlands, 1984.
(30) Jameson, A. K.; Jameson, C. J.; Gutowsky, H. S. *J. Chem. Phys.* **1970**, *53*, 2310.
(31) Jameson, C. J.; Jameson, A. J.; Cohen, S. M. *J. Chem. Phys*. **1975**, *62*, 4424.
(32) Demarquay, J.; Fraissard, J. *Chem. Phys. Lett.* **1987**, *136*, 314.
(33) Roque-Malherbe, R.; Wendelbo, R.; Misfud, A.; Corma, A. *J. Phys. Chem.* **1995**, 14064.
(34) Sastre, G.; Catlow, C. R. A.; Corma, A. *J. Phys. Chem. B* **1999**, *103*, 5187.
(35) Hou, T. J.; Zhu, L. L.; Xu, X. J. *J. Phys. Chem. B* **2000**, *104*, 9356.
(36) Cheung, T. T. P.; Fu, C. M.; Wharry, S. *J. Phys. Chem.* **1988**, *92*, 5170.
(37) Ratcliffe, C. I.; Ripmeester, J. A. *J. Am. Chem. Soc*. **1995**, *117*, 1445.
(38) Ripmeester, J. A.; Ratcliffe, C. I. *Anal. Chim. Acta* **1993**, *283*, 1103.
(39) Larsen, R. G.; Shore, J.; Schmidt-rohr, K.; Emsley, L.; Long, H.; Pines, A.; Janicke, M.; Chmelka, B. F. *Chem. Phys. Lett.* **1993**, *214*, 220.
(40) Mansfeld, M.; Veeman, W. *Chem. Phys. Lett.* **1993**, *213*, 153.
(41) Moudrakovski, I. L.; Ratcliffe, C. I.; Ripmeester, J. A. *Appl. Magn. Reson.* **1995**, *8*, 385; **1996**, *10*, 559.
(42) Pietrass, T.; Kneller, J. M.; Assink, R. A.; Anderson, M. T. *J. Phys. Chem. B* **1999**, *103*, 8837.